Antitumor Activity and Immunostimulant Properties of Liposomes Containing Rosemary Extract on a Mouse Model of Colorectal Cancer

Rouhollah Hemmati Bushehri[1], Mahmoud Reza Jaafari[2], Ghasem Mosayebi[1,3], Ali Ghazavi[1,4], Ali Ganji[1,3*]

[1]Department of Immunology & Microbiology, School of Medicine, Arak University of Medical Sciences, Arak, Iran; [2]Nanotechnology Research Center, Pharmaceutical Technology Institute, Mashhad University of Medical Sciences, Mashhad, Iran; [3]Molecular and Medicine Research Center, Arak University of Medical Sciences, Arak, Iran; [4]Traditional and Complementary Medicine Research Center (TCMRC), Arak University of Medical Sciences, Arak, Iran

ABSTRACT

Background: *Rosemary* (Ros) is a member of the Lamiaceae family known for its antitumor properties. However, its low water solubility and impaired bioavailability are limiting factors when using rosemary extract. Liposomes are synthetic vesicles that offer permeability, improved bioavailability, and lack of immunogenicity and toxicity, making them ideal for delivering various drugs.

Objective: To prepare liposomes (HSPC/Chol/mPEG2000-DSPE) containing rosemary alcoholic extract (LipRos) and evaluate its antitumor properties in a mouse model of colorectal cancer (CRC).

Methods: LipRos were prepared and characterized. CRC was induced in Balb/c mice by subcutaneous injection of C26 cells, and tumor size was monitored continuously. The MTT assay was performed to evaluate cytotoxicity, and liver and kidney function tests were conducted to assess safety. The expression of the pro-apoptotic gene B-cell-lymphoma-2 (Bcl-2), the anti-apoptotic gene Bcl-2-associated-X-protein (Bax), and the expression of cytokines Tumor-necrosis-factor-alpha (TNF-α), Transforming-growth-factor-beta (TGF-β), and Interferon-gamma (IFN-γ) were investigated using real-time PCR. Flow cytometry was used to evaluate the count of cytotoxic (CTL) and regulatory T lymphocytes (Tregs) in spleen and tumor tissue.

Results: The results showed that the size of liposomal formulations and their encapsulation efficiency were 113.4 nm and 85%, respectively. The MTT assay demonstrated insignificant cytotoxicity of LipRos on splenocytes, and the tumor size was significantly reduced in the LipRos group (P=0.00045). LipRos also significantly decreased Bcl-2 gene expression (P=0.0086), increased Bax and IFN-γ gene expression (P=0.031), and enhanced the infiltration of CTLs in tumor tissue (P=0.023).

Conclusion: This study showed that PEGylated (Poly-Ethylene-Glycol) liposomes containing rosemary extract exhibit an antitumor effect on C26 colorectal cancer cells through multiple mechanisms. These findings can be utilized in future studies.

Keywords: Nanoliposomes, Rosemary, Colorectal Cancer, Apoptosis, Cytokine
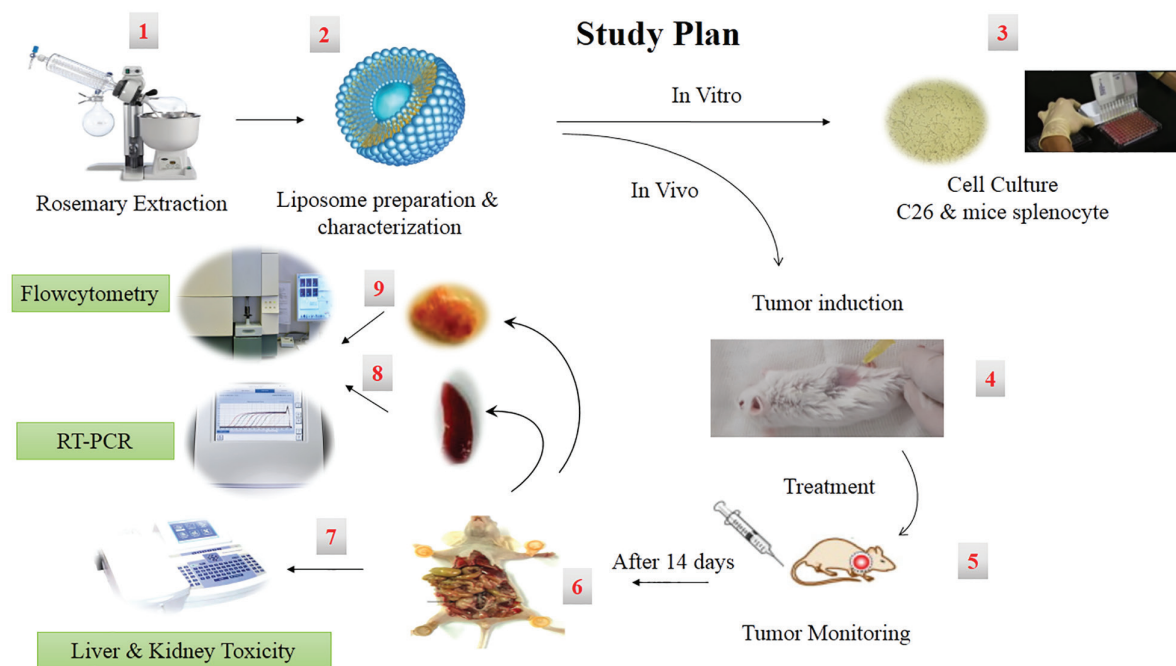
Scheme 1. Graphical Abstract.

INTRODUCTION

Colon cancer is one of the most prevalent cancer diseasees and accounts for one-third of cancer mortality in the population (1). The most common treatment for cancer is chemotherapy; however, it affects healthy cells and has various side effects (2). As a result, complementary therapies such as herbal compounds have been considered.

Among herbal compounds, rosemary is a member of the Lamiaceae family with antioxidant, anti-inflammatory, anti-angiogenic, and antitumor activities (3, 4). Rosemary extract plays a role in fighting tumors by reducing viability in colorectal cancer SW480 and HGUE-C-1cells through cell cycle arrest at G0/G (5). In addition, active compounds in rosemary, such as carnosol, ursolic acid, carnosic acid, rosmarinic acid, and others, exert their anticancer effects through inducing apoptosis, inhibiting prolifration, and preventing metastasis (6-9). For example, rosmarinic acid induces apoptosis in SGC-7901 cells (a line of gastric cancer cells) by increasing the gene expression of Bax and decreasing the gene expression of Bcl-2 (7). Carnosol also induces apoptosis in colon

cancer HCT116 cells by generating ROS (10). Carnosic acid inhibits the metastatic capacity of Caco-2 cells (colorectal cancer) through MMP-9 and MMP-2 gene expression (11). However, challenges such as early degradation, low solubility, and unstable metabolism limit the use of these compounds (12). To solve this problem, the use of nanoparticles such as liposomes is beneficial.

Liposomes are synthetic vesicles with bilayers of phospholipids with amphipathic properties, allowing for the delivery of various hydrophobic and hydrophilic drugs (13). Features such as low toxicity, permeability, adequate bioavailability, and lack of immunogenicity have led to the widespread use of liposomes in drug delivery systems (13). The liposome carries drugs to the tumor site by encapsulating them and releasing their contents into the target cell. Liposomes coated with polyethylene glycol, known as PEGylated liposomes, prevent phagocytosis by the reticuloendothelial (RE) system (13). Using liposomes in the drug delivery system reduces drug toxicity and enhances drug efficacy and stability (14). A study showed that the liposomal form of ursolic acid can modulate regulatory T cells by inhibiting

STAT5 phosphorylation and IL-10 secretion in the breast tumors of mice, leading to a decreased number of MDSCs in the tumor tissue (15). Additionally, it resulted in a higher survival rate in a breast cancer 4T1 mouse model compared to the free form of this substance (16). Although previous studies have shown the therapeutic properties of rosemary alcoholic extract, no studies have been conducted on liposomes containing rosemary alcoholic extract. This study aimed to evaluate the anti-proliferative and antitumor properties of PEGylated liposomes containing rosemary extract on a mouse model and cell line of colorectal cancer.

MATERIALS AND METHODS

Rosemary Extract Preparation

Rosemary leaves were obtained from a local store in Iran and approved by a herbalist expert from Arak University of Medical Sciences. The plant was washed, dried at 25°C, powdered, and then 20 g of rosemary powder was mixed with 200 ml of 99.8 % methanol (absolute) in a 1:10 ratio. Extraction was carried out at 93°C for 4 hours using soxhlation, followed by methanol evaporation at 65°C the rotary evaporators (Laborota 4000, Heidolph, Germany) (17, 18). Rosemary extract (Ros) with a yield of 500 ug/ul was filtered and dried at 37°C. The desired concentration was achieved by dissolving it in dimethyl sulfoxide (DMSO) and then stored at -20°C.

Liposome Preparation and Characterization

Liposomes containing rosemary extract (LipRos) were prepared using the thin-film layer method. Hydrogenated soybean phosphatidyl choline (HSPC) (Ludwigshafen, Germany), cholesterol (Sigma-Aldrich, MO), and mPEG2000-DSPE (Ludwigshafen, Germany) were mixed at a final concentration of 50 mM in a ratio of 65:20:5 mol/mol of HSPC/chol/mPEG2000-DSPE. Additionally, 10% (w/w) rosemary extract was added to

the lipid mixture. The chloroform was evaporated using a rotary evaporator at 40 °C, followed by freeze-drying for 2 hours. Next, the lipid film was hydrated with a 5mM sucrose/histidine buffer at pH=6.5. After hydration, sonication was performed using a bath sonicator (Bandelin, Germany), for 40 minutes at 65°C. To ensure uniform liposome size, the hydrated lipid suspension was passed through filter paper with pore sizes of 400, 200, and 100 nm using an extruder. Finally, the size of the liposome, polydispersity index (PDI), and zeta potential were measured using equipment srom Malvern Instruments Ltd., Malvern, UK. The morphology of the prepared liposomes was also evaluated using atomic force microscopy (AFM).

Determining Encapsulation Efficiency

To determine the encapsulation efficiency percentage (%EE) of rosemary extract in nanoliposomes, a dilution of nanoliposomes was prepared. After lysis using methanol, the liposomes were centrifuged for 10 minutes at 14000g. The released extracts in the supernatant were read at 283 nm. Finally, the encapsulation efficiency was computed using the following formula:
%EE=Extract concentration in liposomes after centrifugation/Extract concentration applied in liposome preparation ×100.

The Release Rate of the Extract

In this study, two buffers (sucrose-histidine with a pH of 6.5 and Phosphate-Buffered Saline (PBS) with a pH of 7.5,) were chosen, 0.5 ml of liposome composition was added to a dialysis bag with a molecular weight cut-off of 3.5 kDa (Pierce, Rockford, IL) and placed in each buffer. Theabsorption of the dialysis buffer was then measured at 283 nm at various time points, including 5, 10, 15, 20, and 30 minutes, as well as 1, 2, 4, 8, 12, 24, and 48 hours.

Cell Culture

The C26 cell line for mouse colon carcinoma was obtained from the Pasteur Institute (Tehran, Iran). For this purpose,

RPMI-1640 medium (Gibco, USA) enriched with 10% fetal calf serum (Gibco, USA), 100 mg/mL streptomycin (Gibco, USA), and 100 U/mL penicillin (Gibco, USA) was used. the cells were then incubated at 37°C in an atmosphere containing 5% CO_2.

Splenocyte Culture

Two mice were sacrificed in accordance with the ethical guidelines outlined by the Ethics Committee of Arak University of Medical Sciences, and were sterilized by immersion in 70% alcohol. The spleen was then excised, and cells from the spleen were perfused using PBS containing 100 mg/mL streptomycin (Gibco, USA), and 100 U/mL penicillin (Gibco, USA). 6 ml of the Ficoll was poured into a Falcon tube, then the cell suspension was gently added to the tube and centrifuged for 15 minutes at 400 g. The splenocytes were collected carefully and cultured in RPMI-1640 medium (Gibco, USA), enriched with 10% fetal calf serum (Gibco, USA), 100 mg/mL streptomycin (Gibco, USA), and 100 U/mL penicillin (Gibco, USA), and then incubated at 37°C in an atmosphere containing 5% CO_2.

MTT Assay

Briefly, $3×10^4/10$ ml of C26 cells were seeded into a 96-well microplate (SPL Life Sciences, Korea) enriched with RPMI-1640 medium, then incubated at 37 °C overnight. Following this, the cells underwent treatment in triplicate for 48 hours at 37°C by increasing the concentrations of Ros and LipRos to 12.5, 25, 50, 100, 200, and 400 µg/mL. Next, 5ug/mL MTT (3-(4, 5-dimethylthiazol-2-yl) -2, 5-diphenyltetrazolium bromide) reagent (Sigma, USA) was added to every well, and after 4 hours of incubation, 100 µl DMSO (Sigma, USA) was added and shaken on a microplate shaker for one hour in the dark. Finally, the absorption was measured using an ELISA reader (Awareness, USA) at 560 nm. The half-maximal inhibitory concentration (IC50) was calculated using Excel with the formula for a linear trend line (Y=mX+c) (Y=viable cell and X=concentration of compound) (19). Based on this calculation, an MTT assay was conducted on mouse spleen cells to assess the cytotoxicity in normal cells.

Animal Model Study

Four week old female BALB/c mice, averaging 22±7 gr in weight, were obtained from the Tehran Pasteur Institute (Iran). They were housed in sterile cages in a light/dark cycle at 22±3°C. The study was initiated following approval from the Ethics Committee of Arak University of Medical Sciences (IR.ARAKMU.REC.1398.337). For tumorinduction, the mice were anesthetized with an intraperitoneal (IP) injection of a ketamine (50 mg/kg) and xylazine (10 mg/kg) mixture. The right flank area of each mouse was selected for the subcutaneous inoculation of $3×10^5$ C26 cells. Following the detection of palpable tumors, the mice received treatment with four intravenous (IV) injections via the tail vein for two weeks (twice a week). The animal groups were treated according to the previous study (18) as follows: LipRos (100 mg/kg/day), Liposomal doxorubicin (Doxil) (2.5 mg/kg/day), Ros (100 mg/kg/day), Doxorubicin (Dox) (2.5 mg/kg/day),, and control (PBS) injection. Tumor size and mice weight were measured during the treatment (Fig. 1). For calculating tumor volume the following formula was used: Tumor volume=length×(width)^2×0.52 (19, 20).

Tumor Tissue and Spleen Excision

The mice were sacrificed after 14 days of treatment, in accordance with the ethical guidelines provided by the Ethics Committee of Arak University of Medical Sciences. The mice were given an intraperitoneal (IP) injection of a ketamine and xylazine mixture, at dosages of 50 mg/kg and 10 mg/kg, respectively. They were then anesthetized, and both tumor tissue and the spleen were excised. Initially, the weight of the excised tumor tissue was measured. Subsequently, the spleen and tumor tissue cells were isolated using a cell strainer (Biofill, UK) (18, 19).
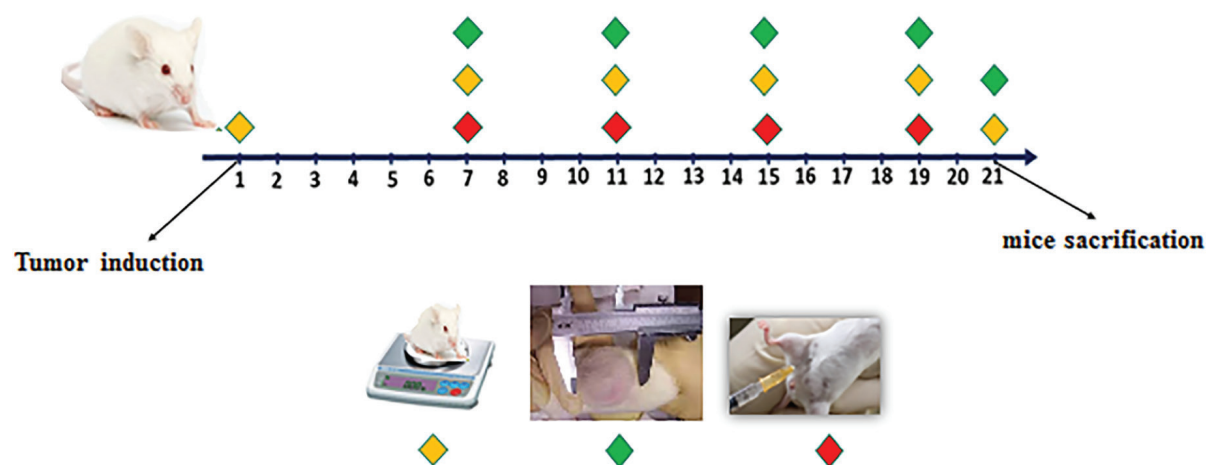
Fig. 1. Study Plan.

Histopathological Assessment of the Tumor

Tumor tissue was excised from mice, fixed in a 10% formalin solution, and embedded in paraffin. Subsequently, sections with a 4 mm thickness were produced and stained with hematoxylin and eosin (H&E). Finally, lymphocyte infiltration in the tumor tissue was investigated based on previous studies (21, 22).

Acute Toxicity Evaluation

Blood specimens were collected from mice hearts to measure serum glutamic pyruvic transaminase (SGPT) and serum glutamic oxaloacetic transaminase (SGOT) (Parsazmoon, Iran) for hepatotoxicity, and creatinine as well as blood urea nitrogen (BUN) (Parsazmoon, Iran) for renal toxicity.

Assay of Gene Expression

The extraction of total RNA from tumor and spleen cells, as well as the synthesis of cDNA, was conducted according to the protocol provided by the manufacturer (Yekta Tajhiz, Iran). Primers sequences for the forward and reverse strands of target genes; Bcl-2 and Bax (apoptotic genes), TNF-α, TGF-β and IFN-γ (cytokine genes), and the reference gene Glyceraldehyde-3-phosphate dehydrogenase (GAPDH) were designed and evaluated using AlleleID 6.0 (Premier Biosoft International, USA), and the BLAST method (Table 1). The real-time PCR assays were performed in a LightCycler 96 Instrument (Roche, Switzerland) using SYBR Green 2x Master Mix (Yekta Tajhiz, Iran) in duplicate. Melting curve assays and

Table 1. The sequence of primers used to evaluate gene expression

Gene	Primers	Length	Sequences, 5′→ 3′
GAPDH	Forward Reverse	224	CGGTGTGAACGGATTTGG CTCGCTCCTGGAAGATGG
Bax	Forward Reverse	174	GCTACAGGGTTTCATCCAG TCCACGTCAGCAATCATCC
Bcl-2	Forward Reverse	161	TGTGGCCTTCTTTGAGTTCG GTTCCACAAAGGCATCCCAG
TNF-α	Forward Reverse	201	CCTCTTCTCATTCCTGCTTGTG ACTTGGTGGTTTGCTACGAC
TGF-β	Forward Reverse	193	AATTCCTGGCGTTACCTTGG GGCTGATCCCGTTGATTTCC
IFN-γ	Forward Reverse	201	AGGAACTGGCAAAAGGATGG GACCTCAAACTTGGCAATACTC

GAPDH: Glyceraldehyde-3-phosphate dehydrogenase; Bax: Bcl-2-associated X protein; Bcl-2: B-cell lymphoma 2; TNF-α: Tumor Necrosis Factor-alpha; TGF-β: Transforming growth factor-beta; IFN-γ: Interferon-gamma

2% gel electrophoresis were used to analyze PCR products, and the absence of nonspecific and primer-dimer products was assessed. In addition, the Pfaffle method was employed to analyze the relative expression of the target genes (23).

Flow Cytometry

Flow cytometry was conducted to immunophenotype T lymphocytes in the spleen and tumor using FACSCalibur (BD Bioscience, CA, USA). To count T regulatory lymphocytes (Treg cells), first 5µl PerCP-conjugated anti-CD25 and PE-conjugated anti-CD4 were first added to the sample and incubated at 25°C for 60 min. Cells were then centrifuged for 5 min at 300G and the supernatant was discarded. Next, 150µl Fixation/Permeabilization buffer (BD Bioscience) was added and incubated at 25°C for 30 minute. Finally, cells were incubated with 5µl FITC-conjugated anti-FoxP3 at 25°C for 30 min. To determine the frequency of Cytotoxic T lymphocytes (CTL), suspended tumor and spleen cells (cell sample) were stained with 5µl PerCP-conjugated anti-CD8 and FITC-conjugated anti-CD3 antibodies and incubated at 25°C for 60 min. Cells were then washed and subjected to flow cytometry.. All antibodies were obtained from eBioscience, USA. For each sample, 10,000 events were acquired on the flowcytometer, and analysis of the results was performed using FlowJo software (Tree Star Inc., OR, USA).

Statistical Analysis

Data was analyzed using SPSS 16.0 software (SPSS, Inc., Chicago, IL, USA). The differences in variables between the groups were evaluated by ANOVA and Tukey's post hoc test. Evaluation of the assumption of normality was performed using the Kolmogorov–Smirnov test. Data are presented as mean±standard deviation (SD) and $P<0.05$ was considered statistically significant.

RESULTS

Liposome Characterization

Fig. 2 displays an image of the prepared liposomes obtained from atomic force microscopy (AFM). The average particle size was 113.4 nm±6.2 (mean±SD), with a PDI indicating a homogeneous distribution of nanoparticles at 0.27±0.012 (mean±SD). Additionally, the results showed that the average zeta potential which contributes to the stability of the liposomal formulation was -10.8±0.59 (mean±SD). The encapsulation efficiency percentage for rosemary extract was 85 %±4.8 (mean±SD), and the amount of extract released was approximately 70 %±3.7 (mean±SD) at pH=6.5 and 31% at pH=7 (Table 2).
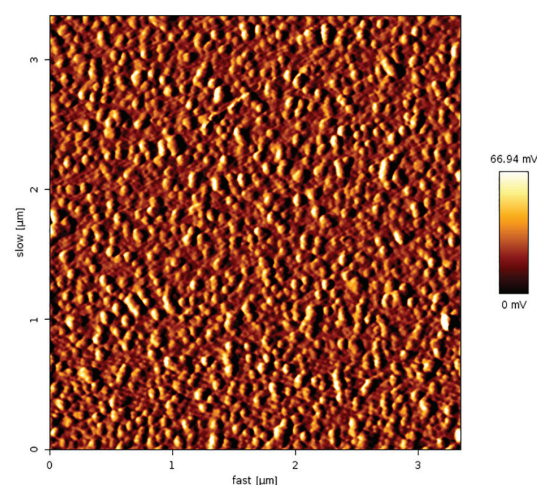

Fig. 2. Atomic force microscopy (AFM) images showed homogeneity of prepared nanoliposomes

Table 2. Characteristics of the prepared liposomes

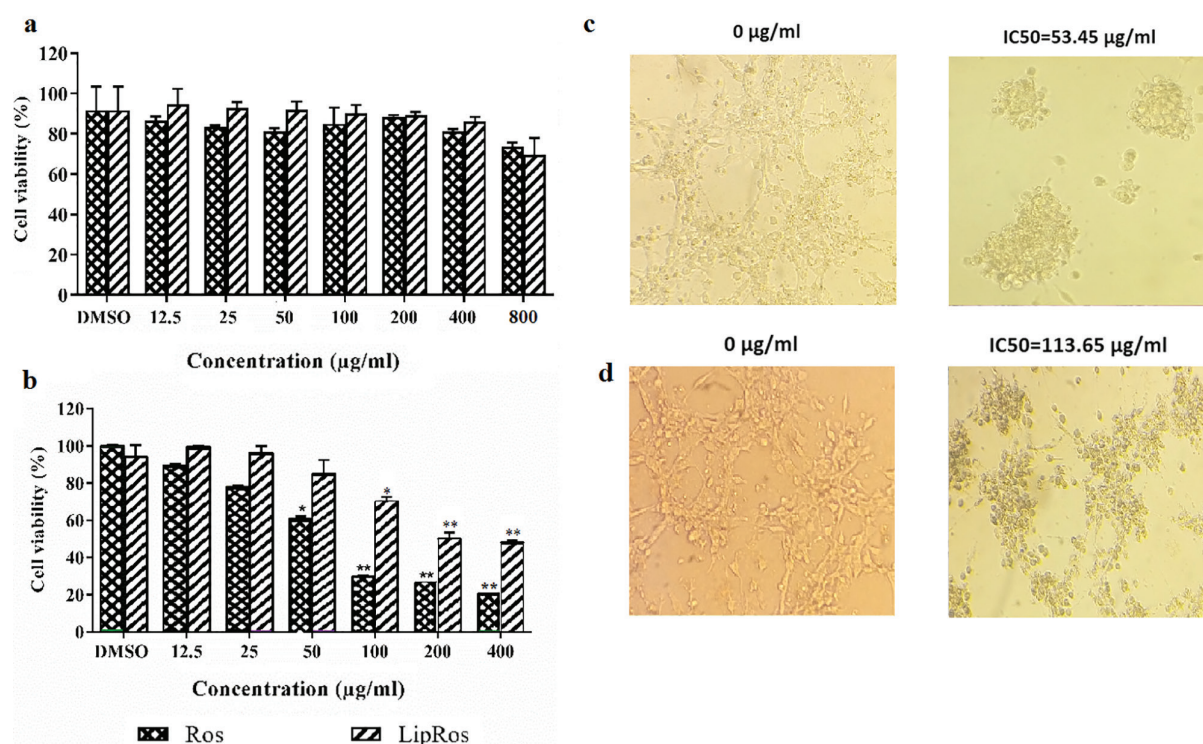| Lipid composition	Molar Ratio (%)	Size (nm) (mean±SD)	PDI (Polydispercity index)	Zeta Potential (mV)	Encapsulation Efficiency (%)	Release Rate (%)
HSPC/Chol/ mPEG2000-DSPE	65:20:5	113.4±6.2	0.27±0.012	-10.8±0.59	85±4.8	70±3.7

Fig. 3. Anti-proliferative effects of LipRos and Ros on mouse splenocytes and C26 cells after 48 hours. (a) The cytotoxic activity of LipRos and Ros at different concentrations on mouse splenocytes compared to DMSO, showed no significant change in cell viability. (b) The cytotoxic effect of LipRos and Ros at different concentrations on C26 cells, compared to DMSO showed a significant reduction in cell viability. (c) 10x microscopic images with the IC50 value in Ros and (d) LipRos treated groups after 48 hours. (*P<0.05, **P<0.01 vs. control). (Ros; Rosemary, LipRos; Liposomal Rosemary)

Evaluation of the Cytotoxicity of LipRos and Ros

The evaluation of the cytotoxic activity of LipRos and Ros compounds on mouse splenocytes (Fig. 3a) shows an insignificant change in cell viability (P>0.05). The effects of the compounds on C26 cell viability showed a significant reduction in the Ros group from 50 µg/mL (P<0.05) and in the LipRos group from 100 µg/mL (P<0.05) compared to DMSO-treated cells (Fig. 3b). The IC50 values were 113.65 µg/mL for LipRos (Fig. 3c) and 53.45 µg/mL for Ros (Fig. 3d).

Antitumor Effects

Tumor size significantly decreased in all treated groups on the 12th and 16th days compared to the control group (P<0.01. Additionally, tumor size significantly reduced on the 20th day of treatment in the Doxil, Ros, and LipRos groups (P<0.001) (Fig. 4a). Moreover, Fig. 4b shows a significant reduction

in tumor weight in the Doxil, Ros, and LipRos groups compared to the control group (P<0.05).

In vivo Cytotoxicity Evaluation

Figs. 5a-d show an insignificant change in the level of SGPT, SGOT, creatinine and BUN in the treatment groups compared to the control group (P>0.05). In addition, an insignificant change was observed in mice weight loss in all treatment groups compared to the control group (P>0.05) (Fig. 5e).

Gene Expression of Bcl-2 and Bax

A significant increase was observed in the gene expression of Bax in the LipRos, Ros, Dox, and Doxil groups compared to the control (P<0.05) (Fig. 6a). On the other hand, LipRos, Dox, and Doxil led to a significant decrease in the expression level of the Bcl-2 gene (P<0.05) (Fig. 6b). Additionally, LipRos significantly reduced the expression level of the Bcl-2 gene compared to the Ros group (P<0.01) (Fig. 6b).
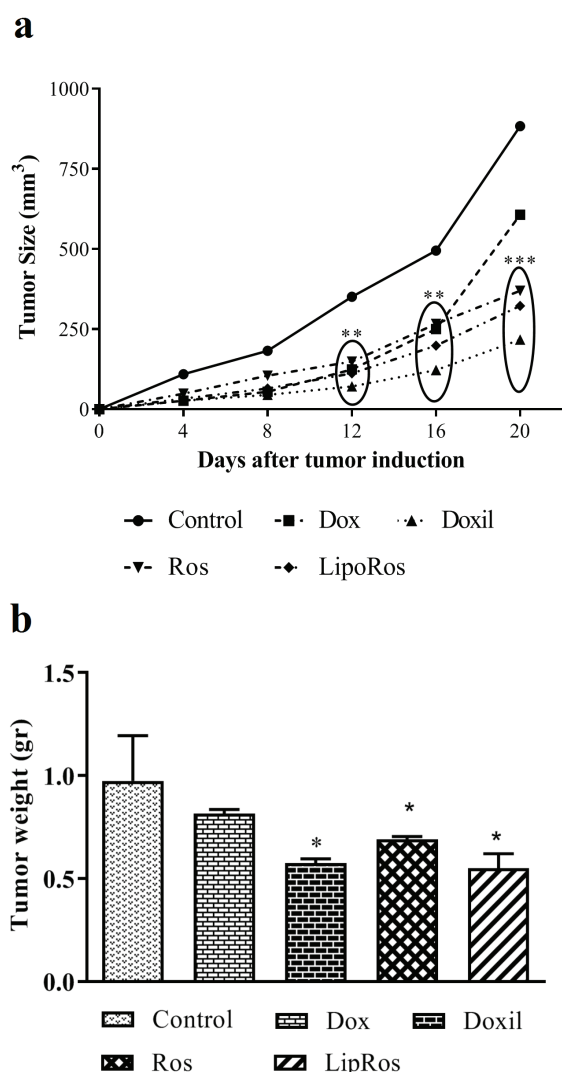
a

b

Fig. 4. Effect of LipRos and Ros on tumor growth in C26 tumor-bearing mice. (a) Doxil, LipRos, and Ros inhibited C26 tumor growth in BALB/c mice. (b) Effect of LipRos and Ros on tumor weight in mice. (*; P<0.05, **; P<0.01; ***;P<0.001 vs. control) (Dox; Doxorubicin, Ros; Rosemary, LipRos; Liposomal Rosemary).

Gene expression of IFN-γ, TGF-β and TNF-α

Doxil and Dox significantly reduced TGF-β gene expression levels (P<0.05) (Fig. 7a). Furthermore, an insignificant change (P>0.05) in TNF-α expression level was observed in any of the treatment groups, compared to the control (Fig. 7b). The results indicated that LipRos and Doxil significantly increased the expression level of IFN-γ (P<0.05) (Fig. 7c).

Tumor Infiltrating Lymphocyte

After preparing tissue sections from the

tumor and histological examination (Fig. 8a), a significant increase in tumor-infiltrating lymphocytes (TILs) was observed in the LipRos group compared to the control group (P<0.01) (Fig. 8b).

Count of CTL and Treg Lymphocytes in Spleen and Tumor

The results of flow cytometry revealed that only the LipRos group significantly increased the frequency of CTLs in tumor tissue compared to the control group (P<0.05) (Fig. 9a). Meanwhile, there were insignificant changes in CTLs in the spleen and Treg cells in both tumor and spleen tissues (P>0.05) (Fig. 9b-d). Figs. 10a-e show the flow cytometry analysis of CTLs and Treg cells.

DISCUSSION

In this study, *Rosmarinus officinalis L.* was extracted using the Soxhlet technique to isolate essential oil containing rosmarinic acid known for its anticancer properties (4, 17). A liposomal formulation was prepared with a composition of HSPC-Chol-mPEG2000-DSPE in which cholesterol stabilized the liposome membrane and PEGylation by mPEG2000-DSPE prevented liposome phagocytosis by the reticuloendothelial system, increasing the circulation of liposomes in the bloodstream for up to 48 hours (13, 24, 25).

The size of the liposome is crucial for delivering the drug to the tumor tissue. Increasing the liposome size by over 200 nm resulted in a decrease in the liposome's half-life and stability, leading to increased liposome clearance. Therefore, liposome sizes in the range of 100 to 150 nm are considered appropriate (26, 27). Consequently, the liposome size and the PDI obtained from the examination of the prepared liposome were suitable for accessing to the tumor and could be effective in successful treatment.

Surface charge or zeta potential is a crucial parameter that influences liposomal behavior,
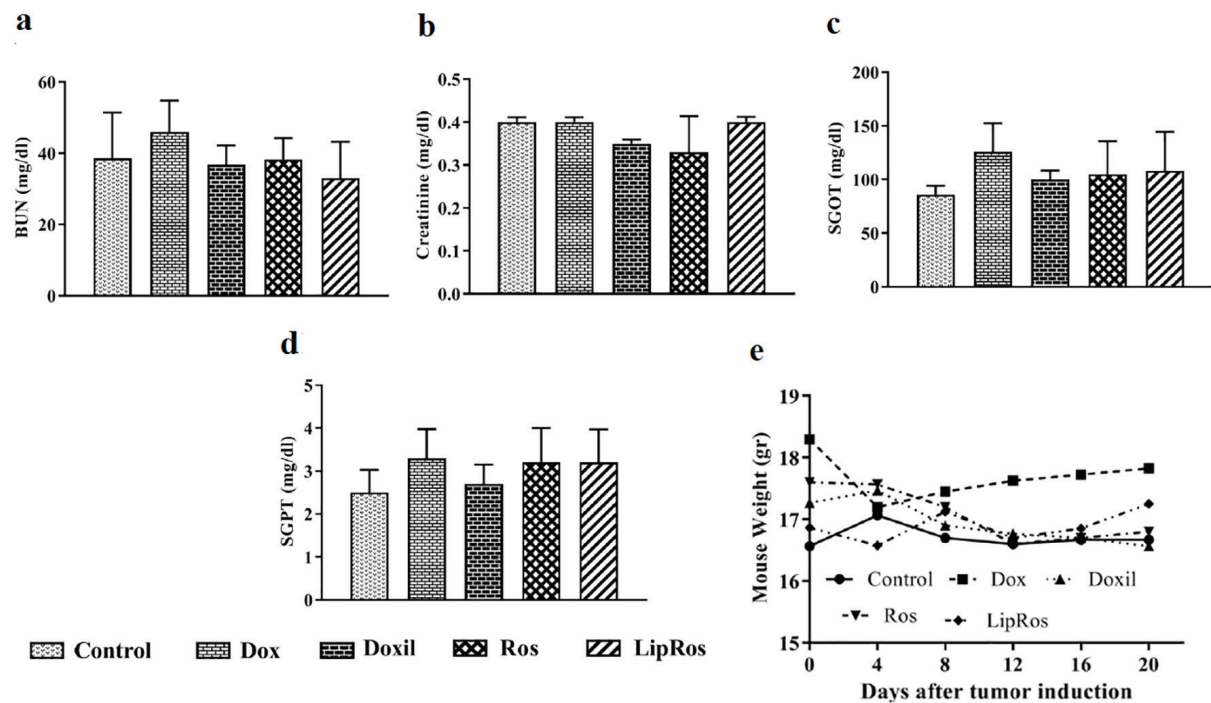
Fig. 5. The effects of LipRos and Ros on liver and kidney function were evaluated by measuring (a) BUN, (b) Creatinine, (c) SGOT, and (d) SGPT levels. (e) The fffect of LipRos and Ros on bodyweight in C26 tumor-bearing mice was insignificant. (P>0.05) (Dox; Doxorubicin, Ros; Rosemary, LipRos; Liposomal Rosemary).
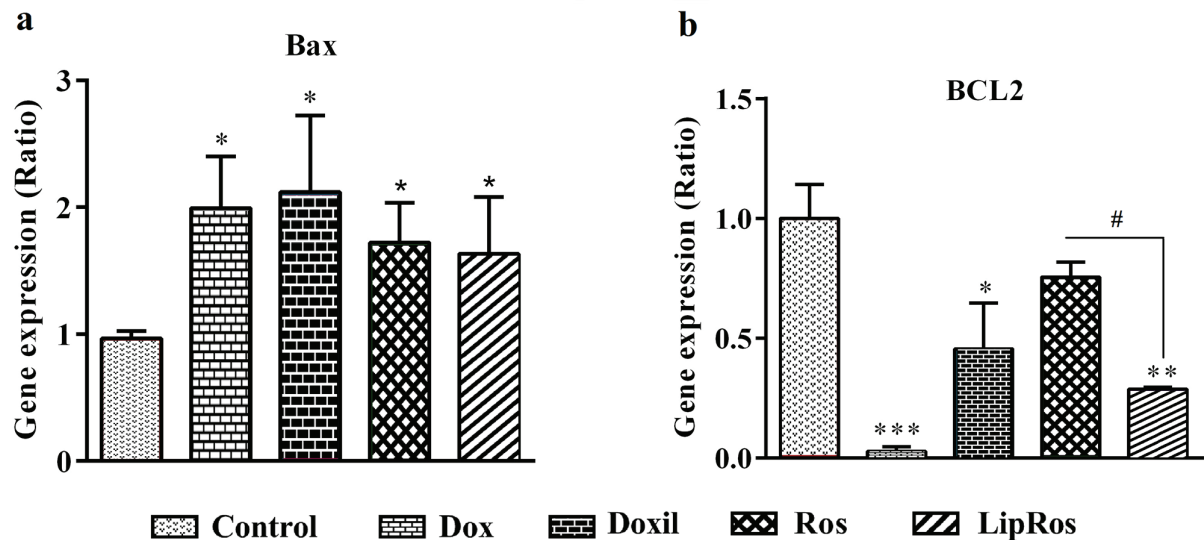

Fig. 6. The expression of Bax and Bcl-2 genes in tumor tissue. (a) Bax gene expression. (b) Bcl-2 gene expression (*; P<0.05, **; P<0.01; ***;P<0.001 vs. control. #; P<0.01 vs. Ros.) (Dox; Doxorubicin, Ros; Rosmary, LipRos; Liposomal Rosemary).

function, and distribution. For instance, in a study by Caldeira de Araujo Lopes et al., it was found that zeta potential values of 30 mV and above helped stabilize liposomal formulations by preventing particle aggregation (27-29). Therefore, as the zeta potential effectively removes liposomes through the reticuloendothelial system, the obtained zeta potential was deemed appropriate and consistent with previous studies (28).

Encapsulation enhances the water solubility, stability, and effectiveness of drugs loaded in liposomes. Theencapsulation efficacy results were similar to the previous studies (25, 29, 30). Release studies indicated that the highest release rate occurs at pH=6.5.
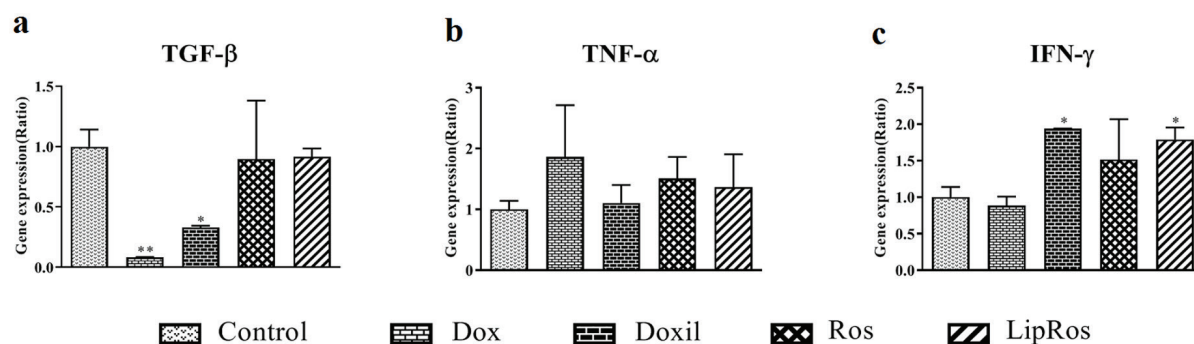
Fig. 7. Gene expression of (a) TGF-β, (b) TNF-α, and (c) IFN-γ. (*; P<0.05, **; P<0.01 vs. control) (Dox; Doxorubicin, Ros; Rosemary, LipRos; Liposomal Rosemary).
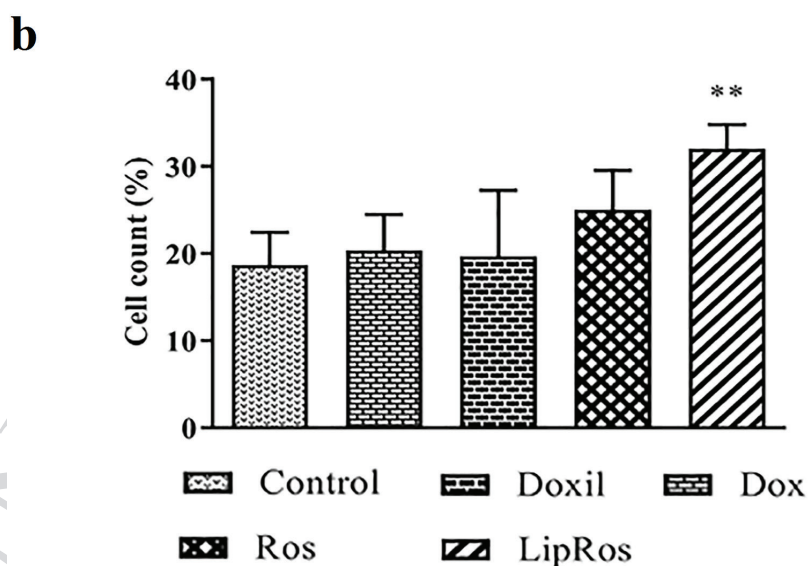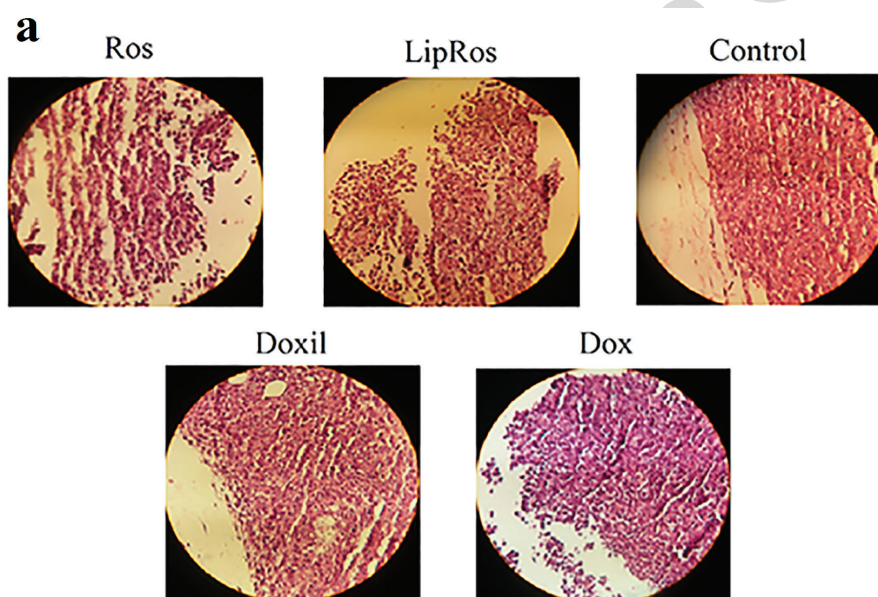

Fig. 8. Evaluation of different treatments on tumor-infiltrating lymphocytes. **(a)** H&E staining of tissue sections taken from colon cancer mice in the Ros, LipRos, Control, Doxil, and Dox treated groups. **(b)** The percentages of tumor-infiltrating lymphocytes in the different treated groups showed a significant increase in the LipRos group. (**; P<0.01 vs. control) (Dox; Doxorubicin, Ros; Rosemary, LipRos; Liposomal Rosemary).
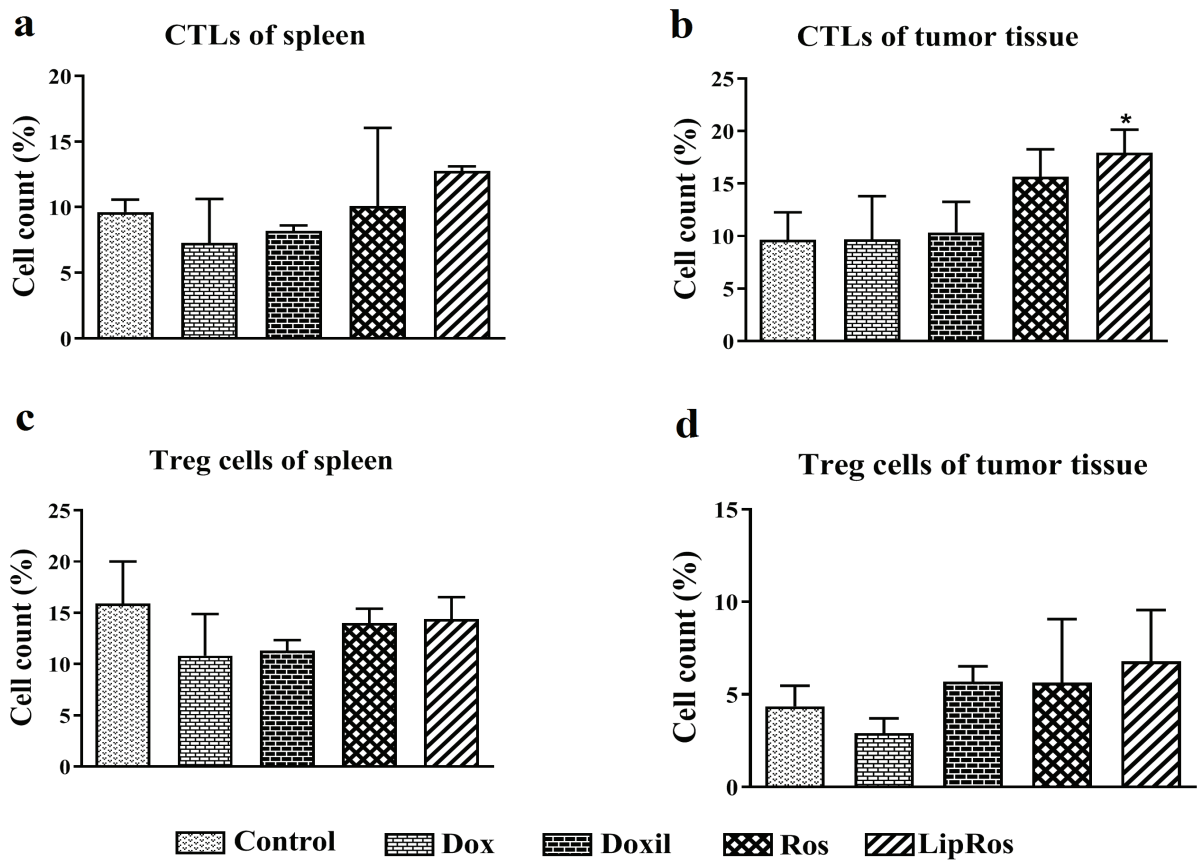
a

CTLs of spleen

b

CTLs of tumor tissue

c

Treg cells of spleen

d

Treg cells of tumor tissue

Control   Dox   Doxil   Ros   LipRos

Fig. 9. Assessment of the cytotoxic and regulatory T lymphocytes in tumor and spleen tissues showed a significant increase in CTLs of tumor tissue in the LipRos group. (a) CTLs in the spleen, (b) CTLs in the tumor, (c) Treg cells in the spleen, (d) Treg cells in the tumor. (*$P<0.05$) (Dox; Doxorubicin, Ros; Rosemary, LipRos; Liposomal Rosemary).

In other words, the acidic conditions of the tumor microenvironment increased the drug release rate from the liposomes (31).

According to the MTT results, LipRos and Ros decreased the viability of C26 cells. However, LipRos showed less cytotoxicity at the same concentrations. This can be explained by the fact that the extract release from liposomes reduced at pH=7.5 compared to free Ros. Furthermore, LipRos and Ros did not affect the viability of mouse splenocytes. This result indicates that LipRos and Ros are not only non-toxic to healthy cells but also have protective effects due to their antioxidant properties (32).

In the treatment groups, insignificant changes were found in mice weight and serum levels of BUN, Creatinine, SGOT, and SGPT. These results indicate the lack of side effects of LipRos on the liver and kidneys, demonstrating the safety of the liposome formulation (18, 29). Furthermore, tumor weight and tumor size significantly decreased in the LipRos and Ros groups, with the greater reduction observed in the LipRos groups, due to liposomal formulation's improved accessibility and longer shelf life at the tumor site (18, 33).

The LipRos and Ros significantly increased Bax gene expression. Although Ros had an insignificant effect on the expression of Bcl-2, LipRos significantly reduced Bcl-2 (anti-apoptotic) gene expression. As mentioned, the impact of LipRos is due to its accumulation in the tumor microenvironment and its greater stability compared to Ros. This may be the reason for increased cell death in treatment groups. These results were consistent with previous studies on rosmarinic acid (9, 18, 34).

The immune-stimulatory effects of LipRos and Ros were evaluated by examining the gene expression of TNF-α, TGF-β, and
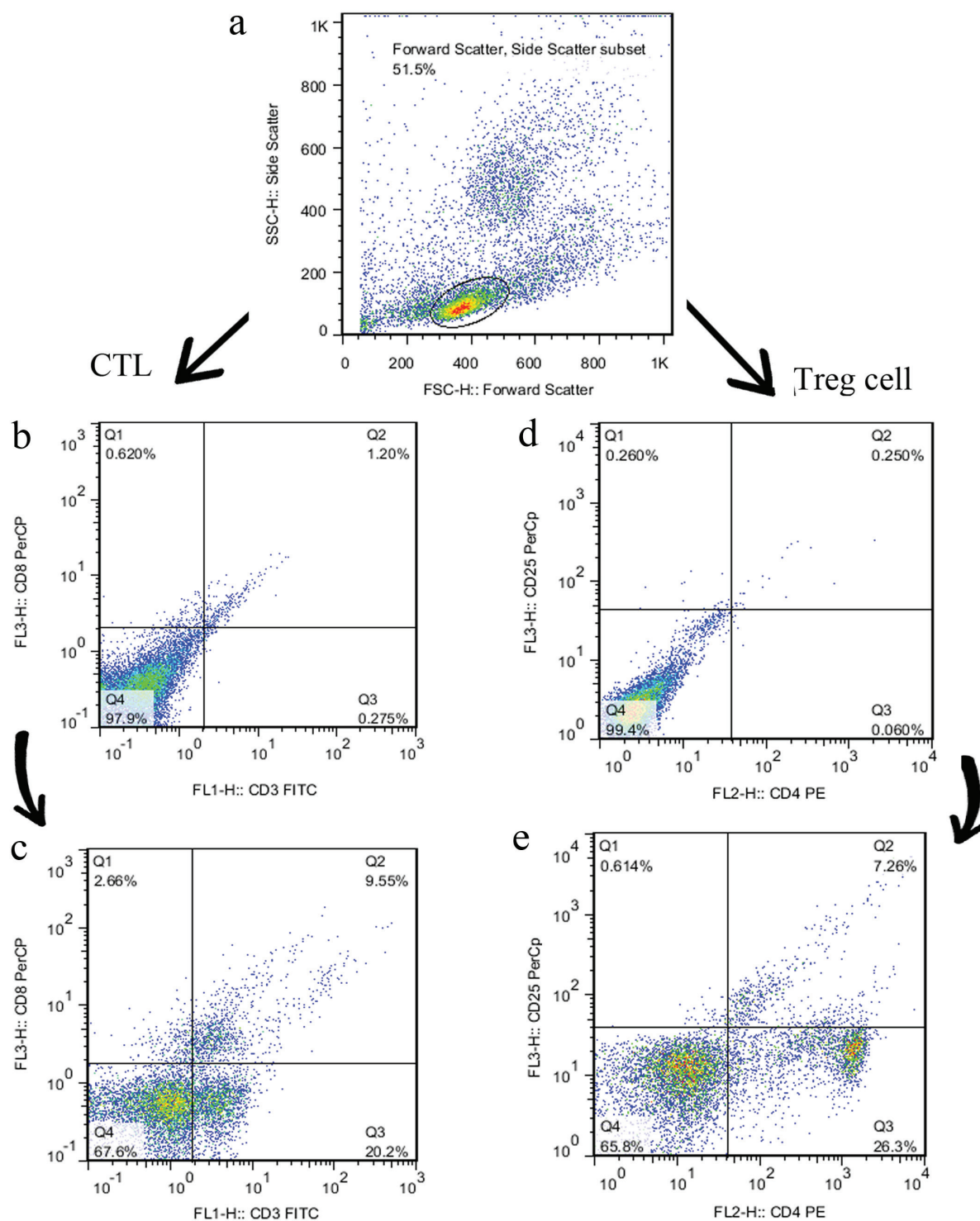
Fig. 10. Flow cytometry diagram of the regulatory and cytotoxic T lymphocytes. (a) Gating of the lymphocyte population. The (b) unstained and (c) stained population of cytotoxic T lymphocytes. The (d) unstained and (e) stained regulatory T lymphocytes.

IFN-γ cytokines. The results showed that LipRos and Ros had an insignificant effect on the expression of TNF-α and TGF-β but significantly increased the gene expression of IFN-γ. This is consistent with previous studies on rosmarinic acid and carnosol (34, 35).

Therefore, LipRos, without reducing TNF-α and TGF-β, enhanced antitumor immunity by increasing IFN-γ expression. In addition to increasing the level of IFN-γ, LipRos may exert its antitumor properties through other mechanisms, such as decreasing the

expression of anti-inflammatory cytokines or increasing the expression of other immunological factors (34, 35) This couls be the focus of the future research.

The histopathological examination of the tumor tissue sections showed that the LipRos group significantly increased tumor-infiltrating lymphocytes (TILs) compared to the control group. However, the other treatment groups did not affect lymphocyte infiltration. In parallel, flow cytometry results revealed that LipRos led to a significant increase in CTLs in tumor tissues, with no changes in Treg cells in tumor tissue or the spleen, and CTLs in the spleen. This result was confirmed by a study on carnosol and carnosic acid (35, 36).

The limitations of this study included evaluating the biodistribution of liposomes, investigating other genes affecting apoptosis, evaluating cell cycle arrest and time constrains that did not allow us to assess other anticancer properties of LipRos.

CONCLUSION

This study demonstrated that LipRos has an antitumor effect on C26 colorectal cancer cells by ebhancing apoptosis and immunostimulant factors. This effect achieved through a significant decrease in Bcl-2 gene expression, significant increase in Bax and IFN-γ gene expression, and enhanced CTL infiltration. The findings suggest that LipRos could serve as a complementary therapy to enhance antitumor properties when used alongside conventional cancer therapies. However, further studies are required to gain insight into the cellular mechanisms and specific molecules that play a role in LipRos's antitumor properties. One of the most important aspects of liposome application is the biodistribution of the liposome which impacts its efficacy and safety. Therefore, future studies can evaluate this parameter and design novel formulation to increase safety and efficacy. Furthermore, researchers can explore the use

of LipRos on other immunological cells and cytokines, different signaling pathways, and in combination with chemotherapy drugs in CRC and other cancers and malignancies.

ACKNOWLEDGMENTS

CONFLICTS OF INTEREST

The authors declare no conflict of interest.

REFERENCES

1. Hashemi F. Colorectal cancer 2019. Available from: https://www.ddri.ir/.
2. Chakraborty S, Rahman T. The difficulties in cancer treatment. Ecancermedicalscience. 2012;6:ed16.
3. Nieto G, Ros G, Castillo J. Antioxidant and Antimicrobial Properties of Rosemary (Rosmarinus officinalis, L.): A Review. Medicines (Basel, Switzerland). 2018;5(3).
4. González-Vallinas M, Reglero G, Ramírez de Molina A. Rosemary (Rosmarinus officinalis L.) Extract as a Potential Complementary Agent in Anticancer Therapy. Nutrition and cancer. 2015;67(8):1221-9.
5. Perez-Sanchez A, Barrajon-Catalan E, Ruiz-Torres V, Agullo-Chazarra L, Herranz-Lopez M, Valdes A, et al. Rosemary (Rosmarinus officinalis) extract causes ROS-induced necrotic cell death and inhibits tumor growth in vivo. Scientific reports. 2019;9(1):808.
6. Vallverdú-Queralt A, Regueiro J, Martínez-Huélamo M, Rinaldi Alvarenga JF, Leal LN, Lamuela-Raventos RM. A comprehensive study on the phenolic profile of widely used culinary herbs and spices: Rosemary, thyme, oregano, cinnamon, cumin and bay. Food Chemistry. 2014;154:299-307.
7. Li W, Li Q, Wei L, Pan X, Huang D, Gan J, et al. Rosmarinic Acid Analogue-11 Induces Apoptosis of Human Gastric Cancer SGC-7901 Cells via the Epidermal Growth Factor Receptor (EGFR)/ Akt/Nuclear Factor kappa B (NF-kappaB)

Pathway. Medical science monitor basic research. 2019;25:63-75.

8. Radziejewska I, Supruniuk K, Nazaruk J, Karna E, Poplawska B, Bielawska A, et al. Rosmarinic acid influences collagen, MMPs, TIMPs, glycosylation and MUC1 in CRL-1739 gastric cancer cell line. Biomedicine & pharmacotherapy = Biomedecine & pharmacotherapie. 2018;107:397-407.

9. Jang YG, Hwang KA, Choi KC. Rosmarinic Acid, a Component of Rosemary Tea, Induced the Cell Cycle Arrest and Apoptosis through Modulation of HDAC2 Expression in Prostate Cancer Cell Lines. Nutrients. 2018;10(11).

10. Park KW, Kundu J, Chae IG, Kim DH, Yu MH, Kundu JK, et al. Carnosol induces apoptosis through generation of ROS and inactivation of STAT3 signaling in human colon cancer HCT116 cells. International journal of oncology. 2014;44(4):1309-15.

11. Barni MV, Carlini MJ, Cafferata EG, Puricelli L, Moreno S. Carnosic acid inhibits the proliferation and migration capacity of human colorectal cancer cells. Oncology reports. 2012;27(4):1041-8.

12. Devi VK, Jain N, Valli KS. Importance of novel drug delivery systems in herbal medicines. Pharmacognosy reviews. 2010;4(7):27-31.

13. Safarzaie A, Beik M, Alizadeh M, Firoozkoohi M. Liposomes and its applications in drug delivery. Nano science and Technology Conference; Gorgan2014.

14. Akbarzadeh A, Rezaei-Sadabady R, Davaran S, Joo SW, Zarghami N, Hanifehpour Y, et al. Liposome: classification, preparation, and applications. Nanoscale research letters. 2013;8(1):102.

15. Zhang N, Liu S, Shi S, Chen Y, Xu F, Wei X, et al. Solubilization and delivery of Ursolic-acid for modulating tumor microenvironment and regulatory T cell activities in cancer immunotherapy. Journal of controlled release : official journal of the Controlled Release Society. 2020;320:168-78.

16. Liu Y, Liu K, Li X, Xiao S, Zheng D, Zhu P, et al. A novel self-assembled nanoparticle platform based on pectin-eight-arm polyethylene glycol-drug conjugates for co-delivery of anticancer drugs. Materials science & engineering C, Materials for biological applications. 2018;86:28-41.

17. Rodríguez-Solana R, Salgado JM, Domínguez JM, Cortés-Diéguez S. Comparison of Soxhlet, Accelerated Solvent and Supercritical Fluid Extraction Techniques for Volatile (GC–MS and GC/FID) and Phenolic Compounds (HPLC–ESI/MS/MS) from Lamiaceae Species. Phytochemical Analysis. 2015;26(1):61-71.

18. Makaremi S, Ganji A, Ghazavi A, Mosayebi G. Inhibition of tumor growth in CT-26 colorectal cancer-bearing mice with alcoholic extracts of Curcuma longa and Rosmarinus officinalis. Gene Reports. 2021;22:101006.

19. Saeedifar AM, Mosayebi G, Ghazavi A, Ganji A. Synergistic Evaluation of Ginger and Licorice Extracts in a Mouse Model of Colorectal Cancer. Nutrition and cancer. 2020:1-11.

20. Baris MM, Serinan E, Calisir M, Simsek K, Aktas S, Yilmaz O, et al. Xenograft tumor volume measurement in nude mice: Estimation of 3D ultrasound volume measurements based on manual caliper measurements. Journal of Basic and Clinical Health Sciences. 2020;4(2):90-5.

21. Zhang D, He W, Wu C, Tan Y, He Y, Xu B, et al. Scoring System for Tumor-Infiltrating Lymphocytes and Its Prognostic Value for Gastric Cancer. Frontiers in immunology. 2019;10:71.

22. Zheng Q, Yang R, Ni X, Yang S, Jiao P, Wu J, et al. Quantitative Assessment of Tumor-Infiltrating Lymphocytes Using Machine Learning Predicts Survival in Muscle-Invasive Bladder Cancer. Journal of Clinical Medicine. 2022;11(23):7081.

23. Pfaffl MW. A new mathematical model for relative quantification in real-time RT-PCR. Nucleic acids research. 2001;29(9):e45.

24. Lamichhane N, Udayakumar TS, D'Souza WD, Simone CB, 2nd, Raghavan SR, Polf J, et al. Liposomes: Clinical Applications and Potential for Image-Guided Drug Delivery. Molecules (Basel, Switzerland). 2018;23(2).

25. Zhao T, Liu Y, Gao Z, Gao D, Li N, Bian Y, et al. Self-assembly and cytotoxicity study of PEG-modified ursolic acid liposomes. Materials science & engineering C, Materials for biological applications. 2015;53:196-203.

26. Maeda N, Takeuchi Y, Takada M, Sadzuka Y, Namba Y, Oku N. Anti-neovascular therapy by use of tumor neovasculature-targeted long-circulating liposome. Journal of controlled release : official journal of the Controlled Release Society. 2004;100(1):41-52.

27. Caldeira de Araujo Lopes S, Vinicius Melo Novais M, Salviano Teixeira C, Honorato-Sampaio K, Tadeu Pereira M, Ferreira LA, et al. Preparation, physicochemical characterization, and cell viability evaluation of long-circulating and pH-sensitive liposomes containing ursolic acid. BioMed research international. 2013;2013:467147.

28. Kateh Shamshiri M, Jaafari MR, Badiee A. Preparation of liposomes containing IFN-gamma and their potentials in cancer immunotherapy: In vitro and in vivo studies in a colon cancer mouse model. Life sciences. 2021;264:118605.

29. Wang M, Zhao T, Liu Y, Wang Q, Xing S, Li L, et al. Ursolic acid liposomes with chitosan modification: Promising antitumor drug delivery and efficacy. Materials science & engineering

C, Materials for biological applications. 2017;71:1231-40.

30. Yücel Ç, Şeker-Karatoprak G. Development and evaluation of the antioxidant activity of liposomes and nanospheres containing rosmarinic acid. Farmacia. 2017;65(1):40-5.

31. Vakili-Ghartavol R, Rezayat SM, Faridi-Majidi R, Sadri K, Jaafari MR. Optimization of Docetaxel Loading Conditions in Liposomes: proposing potential products for metastatic breast carcinoma chemotherapy. Scientific reports. 2020;10(1):1-14.

32. Razavi-Azarkhiavi K, Behravan J, Mosaffa F, Sehatbakhsh S, Shirani K, Karimi G. Protective effects of aqueous and ethanol extracts of rosemary on H2O2-induced oxidative DNA damage in human lymphocytes by comet assay. Journal of complementary & integrative medicine. 2014;11(1):27-33.

33. Mayer LD, Bally MB, Cullis PR, Wilson SL, Emerman JT. Comparison of free and liposome encapsulated doxorubicin tumor drug uptake and antitumor efficacy in the SC115 murine mammary tumor. Cancer letters. 1990;53(2-3):183-90.

34. Cao W, Mo K, Wei S, Lan X, Zhang W, Jiang W. Effects of rosmarinic acid on immunoregulatory activity and hepatocellular carcinoma cell apoptosis in H22 tumor-bearing mice. The Korean journal of physiology & pharmacology : official journal of the Korean Physiological Society and the Korean Society of Pharmacology. 2019;23(6):501-8.

35. Rahnama M, Mahmoudi M, Zamani Taghizadeh Rabe S, Balali-Mood M, Karimi G, Tabasi N, et al. Evaluation of anti-cancer and immunomodulatory effects of carnosol in a Balb/c WEHI-164 fibrosarcoma model. Journal of immunotoxicology. 2015;12(3):231-8.

36. Liu W, Wu TC, Hong DM, Hu Y, Fan T, Guo WJ, et al. Carnosic acid enhances the anti-lung cancer effect of cisplatin by inhibiting myeloid-derived suppressor cells. Chinese journal of natural medicines. 2018;16(12):907-15.